Enhancement of ultrasound on oxidation of AO7 by nZVC peroxomonosulfate combined system

ChaoRong Liu, Jing Zhang, Qingguo Wang, Wei Zhang, Peng Zhou, Sikui Hu and Gucheng Zhang

ABSTRACT

A heterogeneous system using nanoscale zero-valent copper (nZVC) as an activating agent via ultrasound (US) accleration was employed for the degradation of azo dye acid orange 7 (AO7). The degradation rate of AO7 was obviously promoted by ultrasound irradiation as compared to the silent system from 28.83% to 87.39% at 5 min. Via the surface characteristics detected by X-ray photoelectron spectroscopy (XPS), X-ray diffraction (XRD) and scanning electron microscopy (SEM), it was indicated ultrasound can accelerate the corrosion process of nZVC as more Cu^{+} was generated at the same reaction time. Via the particle size detected it was proved US has the ability to disperse the aggregates of nZVC. The addition of neocuproine hemihydrates (NCP) proved Cu^{+} is the primary activating agent and a large number of free radicals (OH• and SO_4^{-}•) were detected by adding methyl alcohol (MA) and tert butyl alcohol (TBA). Then, the parameters investigated were the ultrasound power, acid concentration, and nZVC dosage. The results showed that the increase of ultrasound power has few impacts on AO7 degradation, and with the increase of acid concentration and nZVC dosage, the degradation rate of AO7 was enhanced remarkably. As seen from the above results, it is clear that ultrasound enhances the release of Cu^{+} to participate in the process of AO7 removal.

Key words | acid orange 7, nZVC, PMS, synergistic effect, ultrasound

ChaoRong Liu
Jing Zhang
Qingguo Wang (corresponding author)
Wei Zhang
Peng Zhou
Sikui Hu
Gucheng Zhang
College of Architecture & Environment,
Sichuan University,
Chengdu 610065,
China
E-mail: *wateredu@163.com*

INTRODUCTION

Advanced oxidation processes (AOPs) have emerged as promising technologies to degrade recalcitrant organic contaminants based on the generation of reactive radicals (e.g., sulfate radical (SO_4^{-}•) and hydroxyl radical (OH•)) (Spanggord *et al.* 2000; Rosenfeldt & Linden 2004; Duan *et al.* 2016; Peluffo *et al.* 2016). SO_4^{-}• has gained attention from investigators because it shows a higher redox potential ($E_0 = 2.5–3.1$ V) and SO_4^{-}• can further induce the generation of hydroxyl radical OH• ($E_0 = 1.8–2.7$ V) (House 1962; Chen *et al.* 2012; Fei *et al.* 2014). SO_4^{-}• also has a longer half-life than OH• due to its preference for electron transfer reactions (Anipsitakis & Dionysiou 2004; Furman *et al.* 2010). In general, commonly used oxidants such as peroxomonosulfate (PMS) and persulfate (PS) are applied in the sulfate radicals-based AOPs (Rastogi *et al.* 2009; Nfodzo & Choi 2011; Yuan *et al.* 2011; Guan *et al.* 2013).

In previous research, many transition metal ions have been investigated for the activation of PMS to reactive sulfate radicals (Anipsitakis & Dionysiou 2003, 2004; Bandala *et al.* 2007; Zou *et al.* 2013). It has been reported that Cu^{+} has considerable ability to activate oxidants to produce SO_4^{-}• (Kolthoff & Woods 1966; Masarwa *et al.* 1988; Zhou *et al.* 2016). However, as Cu^{+} is not stable and is easily oxidized to Cu^{2+} by an oxidizing agent in an aqueous solution, Cu^{+}-activated SO_4^{-}• production is seldom reported (Alshamsi & Thomson 2013) Previous studies have shown that zero-valent metal can be a continuous source of low valent metal ions in dissolution

doi: 10.2166/aqua.2018.015

and achieve better catalytic effects (Oh *et al.* 2009; Alshamsi & Thomson 2013; Li *et al.* 2014). In order to solve the difficulty of using Cu^{+}, using nanoscale zero-valent copper (nZVC) can be a potential method of utilizing the generated Cu^{+} during the corrosion process of zero valent copper to activate PMS. However, there are some problems in the use of nanoparticles, such as the aggregates of nanoparticles and the passive film of metal materials (Yan *et al.* 2010).

To solve the problems of using nanoparticles, some attempts have been made regarding the investigation of various combined nano-particles' systems. Since this method is easy to operate, ultrasound (US) has been used as one of the effective technologies for water treatment and has attracted a great deal of attention (Liu *et al.* 2007; Min *et al.* 2012). The mechanism of US can be considered on the basis of the acoustic cavitation in liquid induced by ultrasonic irradiation (Shimizu *et al.* 2007). The collapse of the cavitation bubbles can produce local pressure (1,000 atm) and high temperature (5,000 K) (Suslick 1990; Flint & Suslick 1991). Because nano-materials often aggregate during use, US can dissolve the aggregates of nanoparticles in aqueous solution due to its strong penetrating ability and high energy density (Mondragon *et al.* 2012). In addition, US can destroy the passive film of metallic materials and reduce the particle size through the powerful shear forces in the process of the cavitation bubbles bursting (Wang 2008; Ileri *et al.* 2015). Moreover, US can play a vibratory role, causing similar agitation effects in a heterogeneous system, allowing particles to be more evenly distributed in a solution (Jing *et al.* 2011; Zou *et al.* 2014). Apparently, US has the ability to assist nanoparticles in reaction.

There have been few reports concerning PMS activation by the integrated technology of US and nZVC. Thus, it seems to be significant to introduce ultrasound into the reaction system of nZVC/PMS. The purpose of this work was to investigate the influence of US in a heterogeneous US/nZVC combined system for AO7 degradation. The mechanism of the activation of PMS by heterogeneous US/nZVC composite systems and research on how to degrade AO7 are mainly studied. Finally, the study also discusses the effect of various US power, different pH value, and the change of nZVC dosage in the system.

MATERIALS AND METHODS

Materials

nZVC (size: 10–30 nm, >99.9%), and neocuproine hemihydrate (NCP, >98%) were of analytic purity and obtained from Aladdin Industrial Corporation. Oxone ($KHSO_5{\cdot}0.5KHSO_4{\cdot}0.5\,K_2SO_4$, PMS) and methyl alcohol (MA) were obtained from Sigma-Aldrich. Orange II sodium salt (AO7) was of analytic purity and obtained from Shanghai Macklin Biochemical Co., Ltd. Tert butyl alcohol (TBA), sulfuric acid, and sodium hydroxide were of analytic purity and obtained from Sinopharm Chemical Reagent Co. Ltd, China.

Procedures

Experiments were performed in 500 mL, under constant stirring and constant ultrasonic power. US was furnished by a US generator with frequency of ultrasound (25 kHz) (SB25-12DTD Infinity, Ningbo Xinzhi Biotechnology Co. Ltd). Each 500 mL reaction solution with the desired concentration of AO7 was prepared with ultrapure water and adjusted to the objective initial pH with sulfuric acid and sodium hydroxide, and each run was switched on by adding the desired dosage of PMS and nZVC. MA can then act as an effective quencher for both $SO_4^{-}\bullet$ and OH• because of the high rate constants with $SO_4^{-}\bullet$ ($k = 2.5\times10^{7}\ M^{-1}s^{-1}$) (Neta *et al.* 1988) and OH• ($k = 9.7\times10^{8}\ M^{-1}s^{-1}$) (Buxton *et al.* 1988). TBA is an effective quencher for OH• but not $SO_4^{-}\bullet$, owing to the gap of rate constants with OH• ($k = 6.0\times10^{8}\ M^{-1}s^{-1}$) (Buxton *et al.* 1988) and $SO_4^{-}\bullet$ ($k = 8.0\times10^{5}\ M^{-1}s^{-1}$). The desired TBA and MA were added into the reaction solution before the addition of PMS to identify the primary reactive radicals. NCP was used as Cu(I)-chelation to investigate the role of Cu^{+} in the process and as a kind of chromogenic agent detected by the spectrophotometric method to examine the variation of Cu^{+} concentration in the reaction process (Kim *et al.* 2015). AO7 samples in the process of reaction were withdrawn at set intervals and filtered with a glass fiber membrane (0.45 μm pore size), which can filter out the nZVC catalysts in AO7 samples

leading to the end of the reaction, enabling the AO7 degradation analysis results to be rated accurately.

Sample analysis

The concentration of AO7 was analyzed by UV–vis spectrometer (UV-1800, Shanghai MAPADA Instrument Co., Ltd), equipped with $\lambda = 484$ nm. The particle size of nZVC aggregation was analyzed using particle size analyzer (Accu-SizerTM 780 from Particle Sizing Systems (PSS), Santa Barbara, CA, USA). The pH in aqueous solution was detected by pH meter (Shanghai Leici Apparatus Fac., China). In a previous study, it was proved that Cu^{+} can be chelated with neocuproine, and chromogenic chelate compound would be generated in the process (Larsen 1974). The concentration of Cu^{+} (TCu^{+}) and the total concentration of dissolved copper (TCu) were determined by spectrophotometric method after chelation with NCP, equipped with $\lambda = 454$ nm (UV-1800, Shanghai MAPADA Instrument Co., Ltd).

RESULTS AND DISCUSSION

The experimental phenomenon

Investigation of the US/nZVC/PMS system

The removal of AO7 by US/nZVC/PMS combined system is shown in Figure 1. As can be seen, the reaction balance was reached within 5 min in the US/nZVC/PMS combined system and 87.39% of the initial AO7 was degraded. At the same time, only 28.83% of AO7 removal was obtained in the nZVC/PMS system. It is obvious that the presence of ultrasound can enhance the degradation efficiency of AO7 in the heterogeneous nZVC/PMS system. After 5 min, 13.47 and 1.76% removal of AO7 could be obtained in the US/nZVC and US/PMS system, respectively. It can be seen that the heterogeneous nZVC catalysts and PMS were put to use together in the ultrasound system, which attained greater removal of AO7 than its separated systems.

The effect of US power on the removal of AO7 by the US/nZVC/PMS system was studied in a US range of 200–500 W (Figure 2). It was clear that with an increase in the ultrasonic power from 200 W to 500 W, the degradation

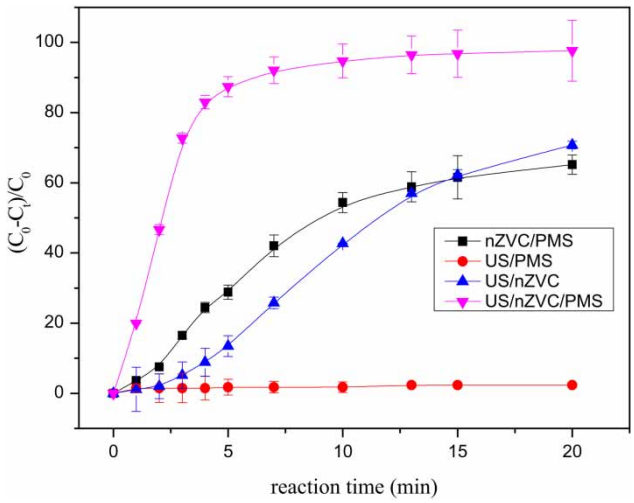

Figure 1 | The effect of ultrasound in AO7 degradation process ($[AO7]_0 = 20$ μM, $[PMS]_0 = 0.4$ mM, $[nZVC]_0$=20 mg·L^{-1}, $pH_0 = 3.0$).

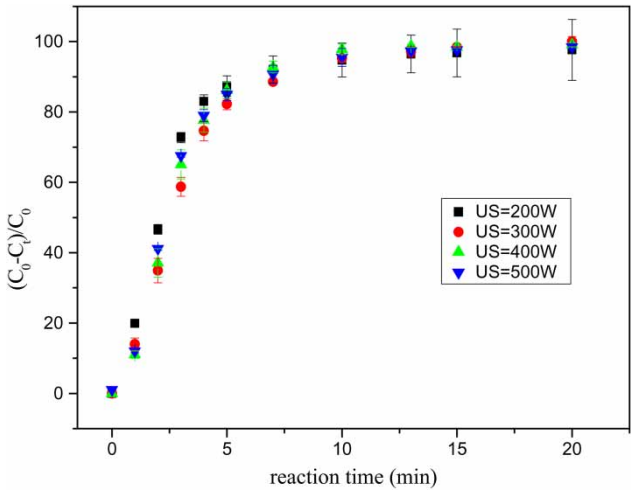

Figure 2 | Effect of different US power on AO7 degradation in the US/nZVC/PMS process ($[AO7]_0 = 20$ μM, $[PMS]_0 = 0.4$ mM, $[nZVC]_0$=20 mg·L^{-1}, US = 200 W, 300 W, 400 W, 500 W, $pH_0 = 3.0$).

ratio of AO7 by the US/nZVC/PMS system was similar within 20 min. It may be considered that there was little influence in the AO7 degradation of the system when US intensity increased. The local high temperature and pressure which were produced by cavitation bubble would accelerate the rate of degradation (Cai *et al.* 2015), but for continuously increased US power, this remarkable benefit was not observed. This was probably because further increase in US power led to the production of an acoustic screen that would terminate the transmission of US in the water, and

this may affect the increase of degradation efficiency of AO7 (Hou *et al.* 2012; Wang *et al.* 2014). The results suggest that the US/nZVC/PMS process could be used to degrade AO7 in the relatively economic ultrasonic power of 200 W.

In general, the results of these research studies illustrate that ultrasound has a great impact on increasing the effect of nZVC catalysts on the activating methods in PMS systems. Limited improvement of the AO7 degradation was observed when the US power was increased from 200 W to 500 W. The activation reaction reached a better result within the shorter time in the presence of the nZVC/PMS under US.

Characterization of nZVC

To obtain the mechanism of the US/nZVC/PMS process, X-ray photoelectron spectroscopy (XPS) spectra, X-ray diffraction (XRD) spectra, and scanning electron microscopy (SEM) images of nZVC before reaction and after reaction at initial pH 3.0 were analyzed. In order to determine the surface chemical composition of nZVC before and after reaction (US/nZVC/PMS system), the XPS measurements of nZVC are shown in Figure 3. In the system, oxygen and copper are the main elements present in the surface of nZVC before and after the reaction. Thus, Cu and O were detected via XPS for exploring the mechanism of reaction. The results showed that all samples have the same ingredient at the surface of nZVC. The XPS results of Cu2p are shown in Figure 3. The peaks at 953.9 eV and 934.0 eV indicate $Cu2p_{1/2}$ and $Cu2p_{3/2}$, respectively (Lu *et al.* 2004; Biesinger *et al.* 2009), and the peaks of the samples indicated that the copper species was Cu^{2+} (Hong *et al.* 2017). In addition, Cu also has two other peaks, 942.7 eV and 962.5 eV, which may be attributed to Cu3d track (Anandan *et al.* 2012). For the XPS results of O as shown in Figure 3, the O peaks for all samples are located at 529.9 eV, 531.4 eV, and 532.8 eV. The positions are respectively assigned to lattice oxygen (M–O), surface hydroxyl oxygen (O–H), and adsorbed H_2O (Lin *et al.* 2016; Peng *et al.* 2016).

nZVC was characterized by XRD and the results are as shown in Figure 4. It was obvious that the two samples have similar results to XRD analysis. The main nZVC structure of both samples before and after the reaction was Cu, with strong diffraction peaks at $2\theta = 43.2°$, 50.2°, and 72.1°. It could be inferred that a little nZVC was oxidized to CuO

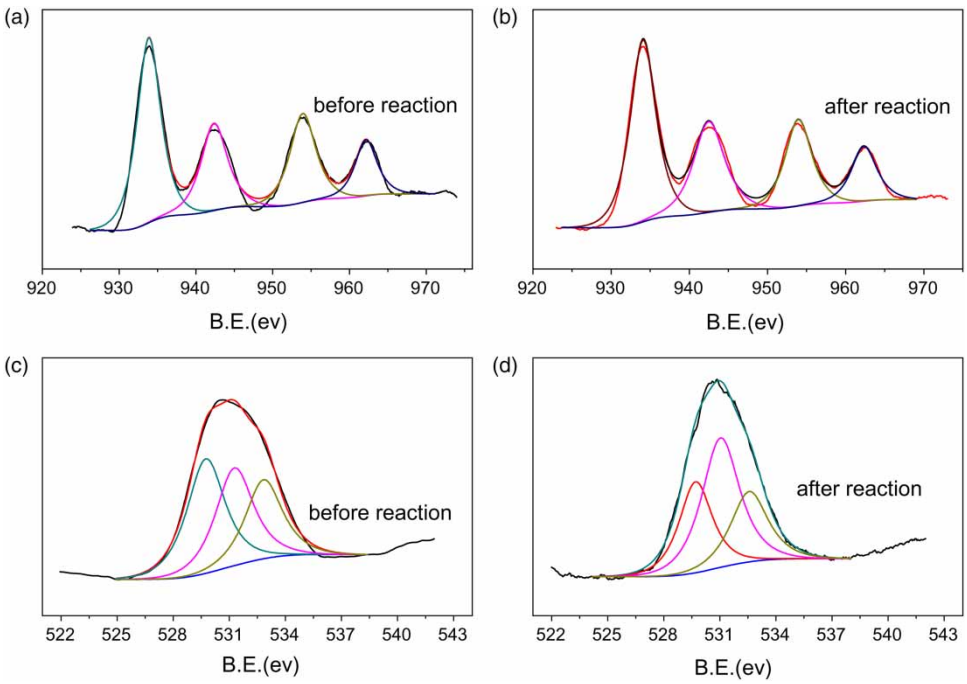

Figure 3 | XPS survey of nZVC before and after reaction in the US/nZVC/PS process and nZVC/PS process: (a) result of Cu before reaction, (b) result of Cu after reaction in US/nZVC/PMS, (c) result of O before reaction, and (d) result of O after reaction in US/nZVC/PMS.

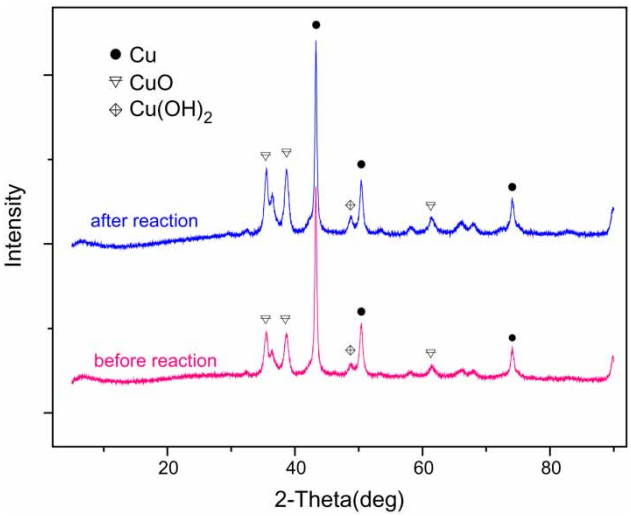

Figure 4 | Diffraction obtained in nZVC characterization by XRD before and after reaction in US/nZVC/PMS.

because of the weak diffraction peaks at $2\theta = 35.3°$, 38.7°, and 48.7°. After the reaction, $Cu(OH)_2$ can be deduced from the results. The results of XPS and XRD indicated that there were almost no changes of the chemical property of nZVC in the process.

The SEM images of nZVC before reaction and after the US/nZVC/PMS process are shown in Figure 5. It is clear that the nZVC before reaction exhibited apparent nano-sized spherical particles, exhibiting larger particle size and slight corrosion in Figure 5(a). In contrast, via the change of particle shape, it can be seen that the surface of nZVC shows visible corrosion after reaction of 2 min in US/nZVC/PMS process, and the nZVC particles become non-spherical, as shown in Figure 5(b). In general, the results proved that the corrosion of nZVC happened in the reaction process, and may indicate that US plays a role in accelerating the speed of nZVC corrosion.

Partical size

For investigating the effect of US on nZVC aggregation, particle sizes from 0.5 μm to 500 μm were used. As can be seen in Figure 6, the main particle size of nZVC was 10 μm to 100 μm before reaction. However, the particle size was 5 μm to 20 μm after reaction at 5 min in the US/nZVC/PMS system, and the main size was 10 μm to 200 μm in the nZVC/PMS system at the same time. It is clear that the main particle size after reaction in the nZVC/PMS system is larger than before the reaction, which means that the nZVC aggregation will be intensified by silent process. But after reaction with US, the aggregation of nZVC was apparently dispersed, and the main particle size was smaller than before reaction. The results indicated that US has strong ability to disperse the aggregates of nZVC to get better effects in the use of nZVC.

Mechanism analysis

The primary reactive radical

The results of the section 'Investigation of the US/nZVC/PMS' indicated that US/nZVC/PMS generated lots of free radicals to degrade AO7 effectively. Based on previous

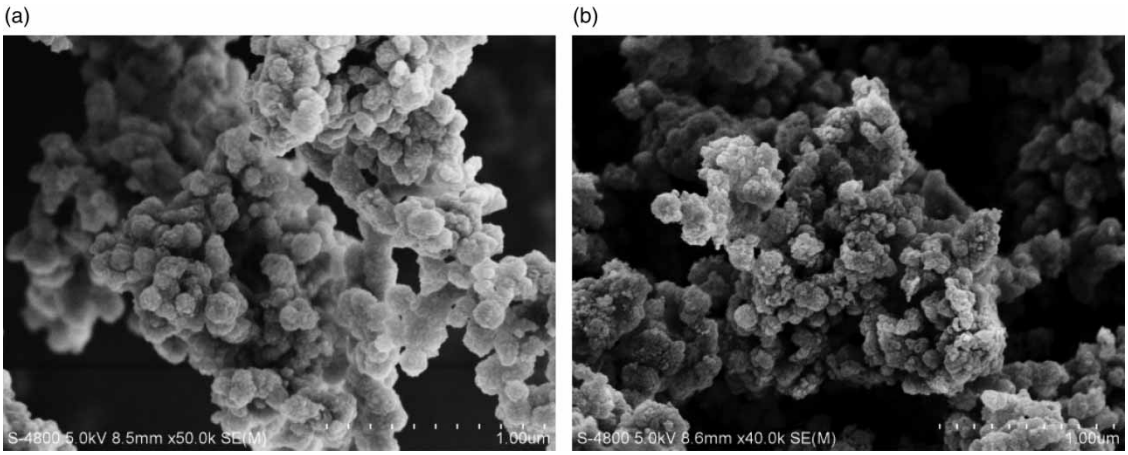

Figure 5 | SEM image of nZVC before (a) and (b) after reaction in the US/nZVC/PS process.

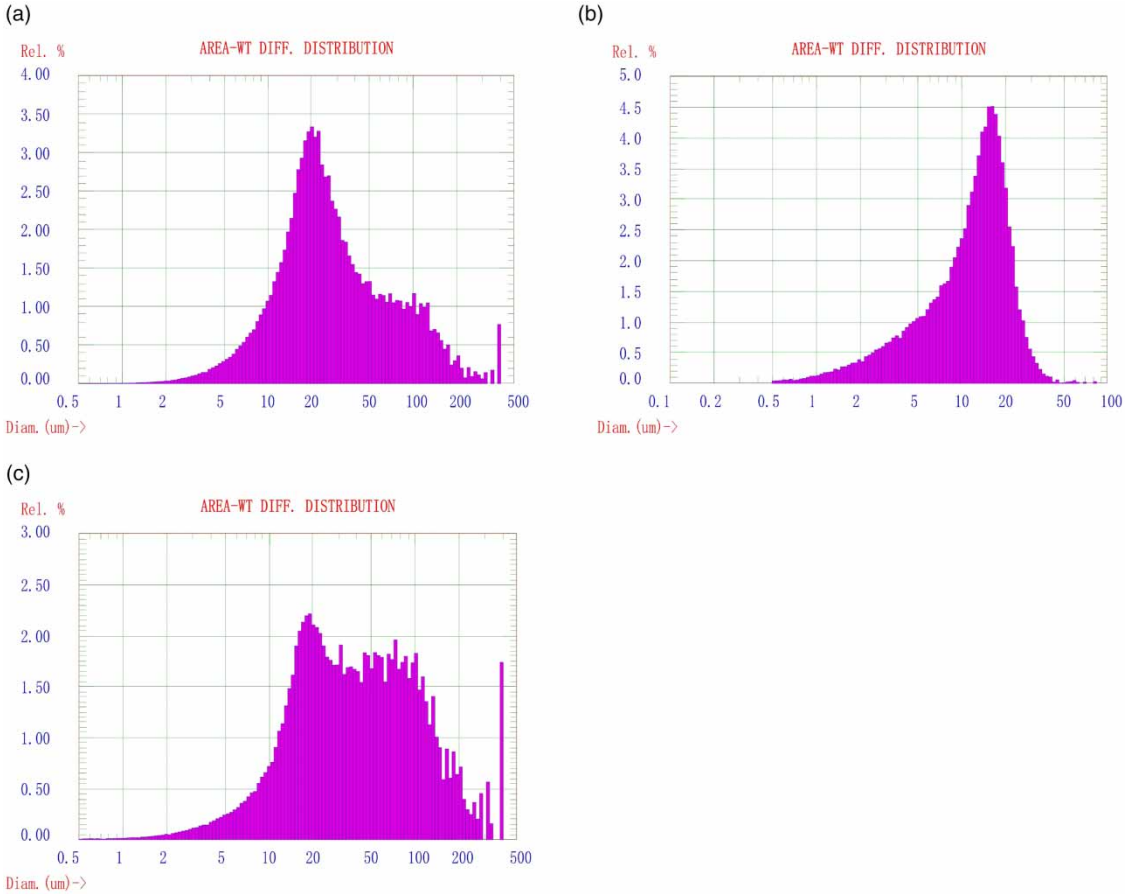

Figure 6 | The particle size of the aggregation of nZVC before (a), after reaction in the US/nZVC/PS process (b), and after reaction in the nZVC/PS process (c) (from 0.5 μm to 500 μm).

studies (Anipsitakis & Dionysiou 2004; Liang & Su 2009), two different reactive radicals, $SO_4^{\bullet-}$ and OH•, may be generated in the process of PMS activation.

After the addition of TBA and MA to the reaction solution, the results of the different system of radicals are shown in Figure 7. It is obvious that the effects were similar with the addition of MA and TBA for the degradation of AO7. After adding in MA and TBA, only about 30% of AO7 removal was obtained in the system in 20 min. It is reasonable to assume that OH• is possibly responsible for the degradation of AO7 in the US/nZVC/PMS system.

Thus, the possible removal mechanisms of AO7 in US/nZVC/PMS systems can be inferred in two ways: (1) the PMS can react with nZVC forming abundant hydroxide radicals, and OH• is the reactant for the degradation of AO7; (2) nZVC was employed as an activator for PMS to generate $SO_4^{\bullet-}$, meanwhile $SO_4^{\bullet-}$ can be quickly transformed to

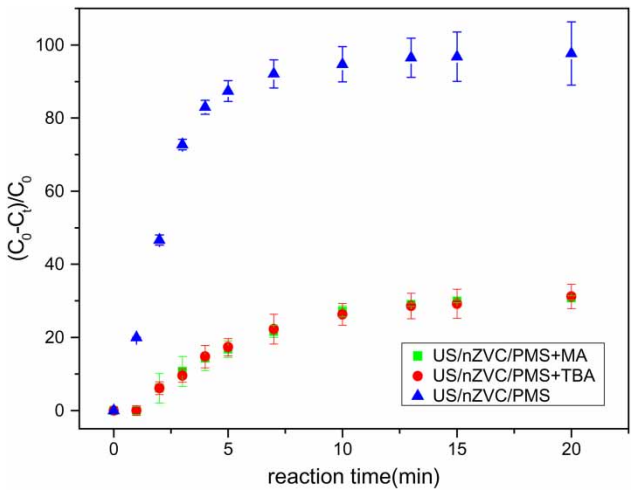

Figure 7 | Inhibition of MA and TBA on AO7 degradation in US/nZVC/PMS process ($[AO7]_0 = 20$ μM, $[PMS]_0 = 0.4$ mM, $[nZVC]_0 = 20$ mg·L^{-1}, $[MA]_0 = [TBA]_0 = 5$ mM, $pH_0 = 3.0$).

OH• via reactions, such as Equation (1) (Furman *et al.* 2010):

$$SO_4^- \bullet + H_2O \rightarrow SO_4^{2-} + OH \bullet + H^+ \quad (1)$$

Major copper species in US/nZVI/PMS system

From the results of nZVC characterization, the corrosion of nZVC happened in the reaction process. A recent study reported that Cu^+ is the major active copper species to activate PMS in an nZVC/PMS system (Zhou *et al.* 2016). With the addition of NCP (a chromogenic agent for Cu^+) in the US/nZVC/PMS process, the concentration of Cu^+ was detected. The result of the concentration of Cu^+ (TCu^+) is presented in Figure 8. In the first 5 min, TCu^+ gradually increased with reaction time, which reached its maximum concentration (1.098 mg/L) and then gradually decreased. This may result from the corrosion of nZVC reaching a higher level.

On account of Cu^+ being quite active, Cu^+ can be rapidly oxidized to Cu^{2+} by oxidizing agents in liquid (Sharma & Millero 1988; Yuan *et al.* 2012). Therefore, detecting the concentration of Cu^{2+} is equally important. The concentration of TCu (including TCu^{2+} and TCu^+) was detected under US and the results are shown in Figure 8. The maximum concentration of TCu under US was 19.96 mg/L in 10 min. In order to compare the effect of US for TCu change in the nZVC/PMS process, TCu change was detected without US and the result presented in Figure 8. The maximum concentration of TCu expected with US was 13.34 mg/L. On the whole, TCu under US has the same consequence as TCu in silent system with the trend rising, but the concentration of Cu becomes lower than before which can indicate US power exists in the US/nZVC/PMS system and accelerates the process of $Cu^0 \rightarrow Cu^+/Cu^{2+}$. To sum up, US has the capacity to promote nZVC corrosion to quicken the speed of AO7 degradation.

NCP can be an effective chelating agent for Cu^+. For verifying the effect of Cu^+ on the process of AO7 depletion, the results of the degradation ratio of AO7 in the presence of NCP are shown in Figure 9. It is clear that the degradation rate of AO7 remarkably declined under NCP – only 10.66% in 20 min. At the same time, degradation of AO7 was completely achieved in the US/nZVC/PMS process, and the ratio of AO7 removal was 97.65%. Based on the intense inhibition of AO7 degradation after adding NCP, the main activating ingredient to activate PMS should be Cu^+ in the US/nZVC/PMS system.

It is often necessary to consider the impact of adsorption on the concentration of pollutant for nano-materials participating in the experimental process (Wang *et al.* 2017, 2018). On the basis of the results of TCu in Figure 6, the concentration of total Cu was about to reach 20 mg/L. Contrasted with the initial nZVC dosage (20 mg/L), it can be assumed that nZVC is almost completely dissolved so the effect of

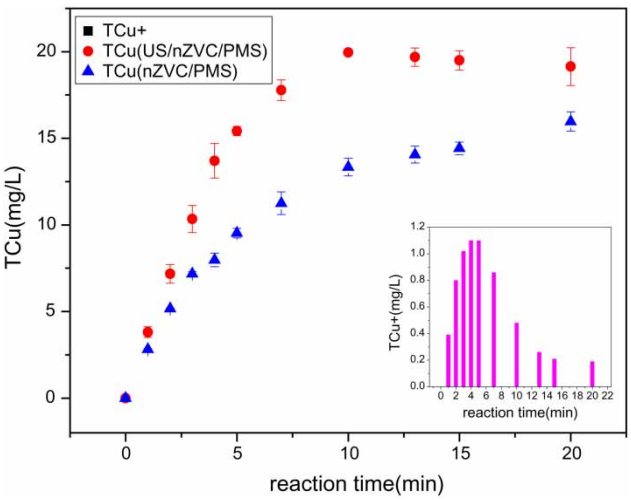

Figure 8 | TCu^+, TCu and the effect of US of TCu ($[AO7]_0 = 20$ μM, $[PMS]_0 = 0.4$ mM, $[nZVC]_0 = 20$ mg·L^{-1}, $[NCP]_0 = 1$ mM, US = 200 W, $pH_0 = 3.0$).

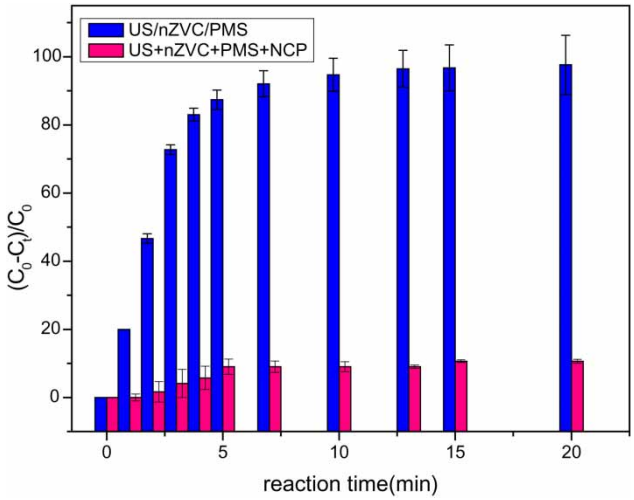

Figure 9 | The effect of NCP on AO7 degradation in the US/nZVC/PMS process ($[AO7]_0 = 20$ μM, $[PMS]_0 = 0.4$ mM, $[nZVC]_0 = 20$ mg·L^{-1}, $[NCP]_0 = 1$ mM, $pH_0 = 3.0$).

adsorption can be considered small in the US/nZVC/PMS system.

When PMS activation is considered with respect to Cu^+ consumption, the benefit of ultrasound in the heterogeneous nZVC/PMS system is evident in accelerating the release of Cu^+ and the reactions probably occur in the solutions below (Equations (2) and (3)). All in all, according to the experimental results above, the mechanism of degradation of AO7 may involve the reactions as follows (Equations (4)–(7)). The mechanism of the US/nZVC/PMS process is shown in Figure 10.

$$Cu^0_{(s)} + \frac{1}{2}H_2O \overset{US}{\rightarrow} Cu^+ + \frac{1}{2}OH^- + H_2 \ (US\ promote\ the\ dissolution) \quad (2)$$

$$Cu^0_{(s)} + \frac{1}{2}HSO_5^- \overset{US}{\rightarrow} Cu^+ + \frac{1}{2}OH^- + \frac{1}{2}SO_4^{2-} \ (US\ promote\ the\ dissolution) \quad (3)$$

$$Cu^+ + HSO_5^- \rightarrow Cu^{2+} + OH^- + SO_4^-\bullet \quad (4)$$

$$Cu^+ + HSO_5^- \rightarrow Cu^{2+} + SO_4^{2-} + OH\bullet \quad (5)$$

$$Cu^{2+} + HSO_5^- \rightarrow Cu^+ + SO_5^-\bullet + H^+ \quad (6)$$

$$AO7\ solution + SO_4^-\bullet + OH\bullet \rightarrow small\ organic\ and\ inorganic\ compounds \quad (7)$$

Effect of initial pH

Different initial solutions of pH were investigated to evaluate their effect on AO7 removal with the US/nZVC/PMS treatment systems. Figure 11 presents time-dependent changes of the concentration of AO7 in US/nZVC/PMS systems during different initial solution pH. The final removal efficiency of AO7 under pH = 2, 3, 4, 5 over a 20 min reaction time was 100%, 97.65%, 77.78%, and 61.69%, respectively. According to the results, during increase of the pH solution, a lower degrading effect was obtained for AO7. The degradation experiments performed a quicker reaction at pH less than or equal to 3 and the chemical reaction equilibrium was reached around 5 min. At the same reaction time, the AO7 degradation was only 26.35% and 22.40% at pH 4 and 5. Moreover, the results of experiments in 0–5 min fitted with the pseudo-first-order kinetic model, and the degradation rate of AO7 was respectively 7.75×10^{-3} min^{-1} ($R^{2=}$0.98703), 6.08×10^{-3} min^{-1} ($R^{2=}$0.96296), 4.4777×10^{-1} min^{-1} ($R^{2=}$0.97711), and 5.9939×10^{-1} min^{-1} ($R^{2=}$0.99345) in pH at 2, 3, 4, and 5. It was clear that a higher reaction rate can be gained at lower pH value. The results suggest that the US/nZVC/PMS treatment process can be used to degrade AO7 at pH below 3 which can promote the corrosion of nZVC to release Cu^+, which is the major activating product.

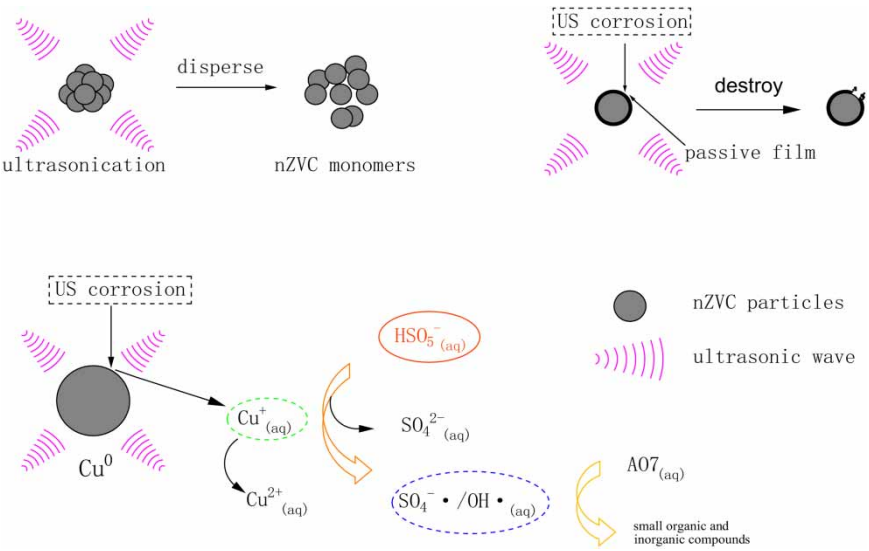

Figure 10 | The mechanism of the US/nZVC/PMS process.

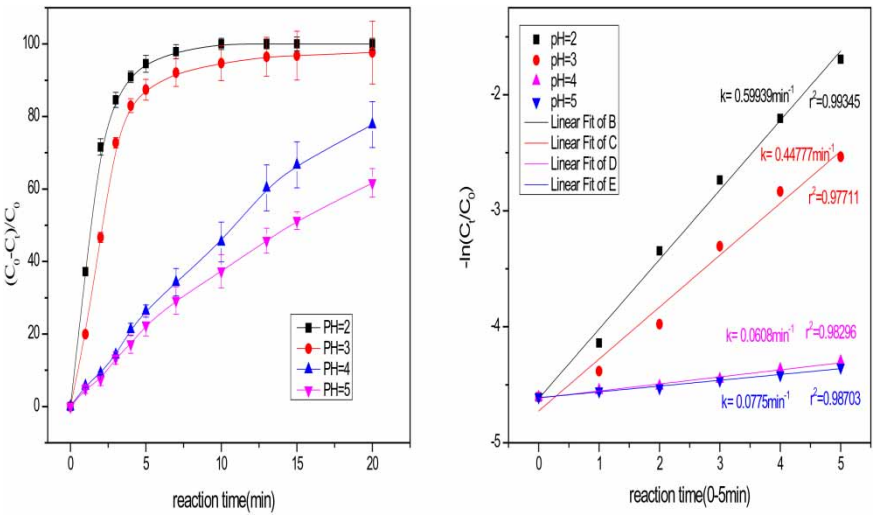

Figure 11 | Effect of different PH on AO7 degradation in US/nZVC/PMS process ($[AO7]_0 = 20\ \mu M$, $[PMS]_0 = 0.4$ mM, $[nZVC]_0 = 20\ mg{\cdot}L^{-1}$, US = 200 W, $PH_0 = 2.0, 3.0, 4.0, 5.0$).

Effect of nZVC dosage

In order to assess the impact of the nZVC dosage on the AO7 removal by the US/nZVC/PMS treatment system, experiments were conducted with 20 μmg/L aqueous AO7 solutions in the presence of a series of concentration of nZVC at pH 3, as shown in Figure 12. The AO7 removal obviously increased for different concentrations of the nZVC (5 mg/L, 10 mg/L, 20 mg/L, 30 mg/L, 40 mg/L) system and respectively were 73.75%, 89.85%, 97.65%, 98.50%, 97.30% after reaction time of 20 min. Enhancement of the degradation rate could be attributed to more Cu^{+} being released to induce a larger number of reactive radicals and more active sites on the surface of the nZVC when the dosage of nZVC increased. Moreover, the results of different nZVC doses in 0–5 min fitted with the pseudo-first-order kinetic model, and the AO7 degradation rate was respectively $1.3906 \times 10^{-1}\ min^{-1}$ (R^2=0.91231), $2.9139 \times 10^{-1}\ min^{-1}$ (R^2=0.94367), $4.4777 \times 10^{-1}\ min^{-1}$ (R^2=0.97711), $4.3365 \times 10^{-1}\ min^{-1}$ (R^2=0.98842), and $5.8089 \times 10^{-1}\ min^{-1}$ (R^2=0.98747) at nZVC dosage of

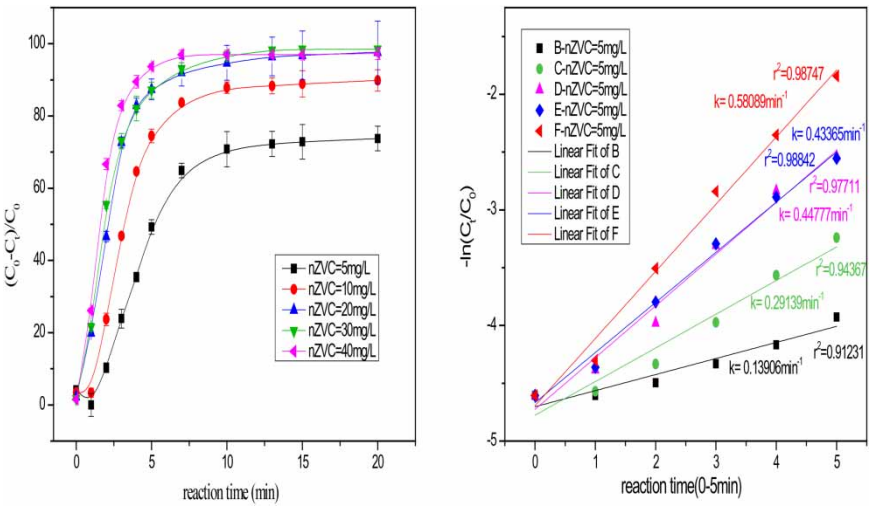

Figure 12 | Effect of different nZVC dosages on AO7 degradation in US/nZVC/PMS process ($[AO7]_0 = 20\ \mu M$, $[PMS]_0 = 0.4$ mM, $[nZVC]_0 = 5\ mg{\cdot}L^{-1}$, $10\ mg{\cdot}L^{-1}$, $20\ mg{\cdot}L^{-1}$, $30\ mg{\cdot}L^{-1}$, $40\ mg{\cdot}L^{-1}$, US = 200 W, $pH_0 = 3.0$).

5 mg/L, 10 mg/L, 20 mg/L, 30 mg/L, 40 mg/L. Nevertheless, based on the results, a tiny increase of AO7 degradation in the nZVC dosage from 20 mg/L to 40 mg/L was observed.

CONCLUSION

All data collected here for the degradation of AO7 demonstrated the importance of identifying the impact of ultrasound on nZVC/PMS systems.

The mechanism investigation shows that ultrasound was proven to have the capacity to accelerate the speed of nZVC corrosion and disperse aggregates of nZVC, and Cu^{+} was generated in the process. Cu^{+} is the primary activating agent to activate PMS, producing a large number of free radicals (OH• and SO_4^{-}•) that can degrade AO7 effectively. The percentage AO7 degradation depended on the US power, pH solution, and nZVC dosage, and results suggested selecting the initial pH at 3.0, US power at 200 W, and nZVC dosage at 20 mg/L. As a result, we can suggest that ultrasound-assisted nZVC and PMS is a suitable technique for the remediation of AO7 contaminated water.

The results provide valuable information with regard to the treatment of azo dye wastewaters. US/nZVC/PMS acidic systems possess remarkable oxidation capacity for pollutants. Possible future studies could investigate different ways to enhance the efficiency of PMS activation or increase the speed of nZVC corrosion in nZVC/PMS systems and investigate more convenient, cheap, and clean methods of practical use.

ACKNOWLEDGEMENTS

Appreciation and acknowledgment are given to the National Key Research and Development Program of China (2016YFC0401710).

REFERENCES

Alshamsi, M. A. & Thomson, N. R. 2013 Treatment of organic compounds by activated persulfate using nanoscale zerovalent iron. *Industrial & Engineering Chemistry Research* **52**, 13564–13571.

Anandan, S., Lee, G. J. & Wu, J. J. 2012 Sonochemical synthesis of CuO nanostructures with different morphology. *Ultrasonics Sonochemistry* **19**, 682–686.

Anipsitakis, G. P. & Dionysiou, D. D. 2003 Degradation of organic contaminants in water with sulfate radicals generated by the conjunction of peroxymonosulfate with cobalt. *Environmental Science & Technology* **37** (20), 4790–4797.

Anipsitakis, G. P. & Dionysiou, D. D. 2004 Radical generation by the interaction of transition metals with common oxidants. *Environmental Science & Technology* **38** (13), 3705–3712.

Bandala, E. R., Pelaez, M. A., Dionysiou, D. D., Gelover, S., Garcia, J. & Macias, D. 2007 Degradation of 2,4 dichlorophenoxyacetic acid (2,4-D) using cobalt-peroxymonosulfate in Fenton-like process. *Journal of Photochemistry and Photobiology A-Chemistry* **186** (2–3), 357–363.

Biesinger, M. C., Payne, B. P., Lau, L. W. M., Gerson, A. & Smart, R. St. C. 2009 X-ray photoelectron spectroscopic chemical state quantification of mixed nickel metal, oxide and hydroxide systems. *Surface & Interface Analysis* **41** (4) 324–332.

Buxton, G. V., Greenstock, C. L., Helamn, W. P. & Ross, A. B. 1988 Critical review of rate constants for reactions of hydrated electrons, hydrogen atoms and hydroxyl radicals (•OH/•O^{-} in aqueous solution. *Journal of Physical & Chemical Reference Data* **17** (2), 513–886.

Cai, C., Zhang, H., Zhong, X. & Hou, L. . 2015 Ultrasound enhanced heterogeneous activation of peroxymonosulfate by a bimetallic Fe-Co/SBA-15 catalyst for the degradation of Orange II in water. *Journal of Hazardous Materials* **283**, 70–79.

Chen, L., Peng, X., Liu, J., Li, J. & Wu, F. 2012 Decolorization of Orange II in aqueous solution by an Fe(II)/sulfite system: replacement of persulfate. *Industrial & Engineering Chemistry Research* **51** (42), 13632–13638.

Duan, X., Su, C., Zhou, L., Sun, H., Suvorova, A., Odedairo, T., Zhu, Z., Shao, Z. & Wang, S. 2016 Surface controlled generation of reactive radicals from persulfate by carbocatalysis on nanodiamonds. *Applied Catalysis B-Environmental* **194**, 7–15.

Fei, Q., Wei, C. & Bingbing, X. 2014 Modeling the heterogeneous peroxymonosulfate/Co-MCM41 process for the degradation of caffeine and the study of influence of cobalt sources. *Chemical Engineering Journal* **235**, 10–18.

Flint, E. B. & Suslick, K. S. 1991 The temperature of cavitation. *Science* **253** (5026), 1397–1399.

Furman, O. S., Teel, A. L. & Watts, R. J. 2010 Mechanism of base activation of persulfate. *Environmental Science & Technology* **44** (16), 6423–6428.

Guan, Y., Ma, J., Ren, Y., Liu, Y., Xiao, J., Lin, L. & Zhang, C. 2013 Efficient degradation of atrazine by magnetic porous copper ferrite catalyzed peroxymonosulfate oxidation via the formation of hydroxyl and sulfate radicals. *Water Research* **47** (14), 5431–5438.

Hong, R., Guo, Z., Gao, J. & Gu, C. 2017 Rapid degradation of atrazine by hydroxyl radical induced from montmorillonite templated subnano-sized zero-valent copper. *Chemosphere* **180**, 335–342.

Hou, L., Zhang, H. & Xue, X. 2012 Ultrasound enhanced heterogeneous activation of peroxydisulfate by magnetite catalyst for the degradation of tetracycline in water. *Separation and Purification Technology* **84** (SI), 147–152.

House, D. A. 1962 Kinetics and mechanism of oxidations by peroxydisulfate. *Chemical Reviews* **62** (3), 185–203.

Ileri, B., Ayyildiz, O. & Apaydin, O. 2015 Ultrasound-assisted activation of zero-valent magnesium for nitrate denitrification: Identification of reaction by-products and pathways. *Journal of Hazardous Materials* **292**, 1–8.

Jing, G., Zhou, Z., Song, L. & Dong, M. 2011 Ultrasound enhanced adsorption and desorption of chromium (VI) on activated carbon and polymeric resin. *Desalination* **279** (1–3), 423–427.

Kim, H., Nguyent, T., Lee, H. & Lee, C. 2015 Enhanced inactivation of Escherichia coli and MS2 coliphage by cupric ion in the presence of hydroxylamine: dual microbicidal effects. *Environmental Science & Technology* **49** (24), 14416–14423.

Kolthoff, I. M. & Woods, R. 1966 Polarographic kinetic currents in mixtures of persulfate and copper(II) in chloride medium. *Journal of the American Chemical Society* **88**, 1371–1375.

Larsen, E. R. 1974 Spectrophotometric determination of copper in fertilizer with neocuproine. *Analytical Chemistry* **46** (8), 1131–1132.

Li, H., Wan, J., Ma, Y., Wang, Y. & Huang, M. 2014 Influence of particle size of zero-valent iron and dissolved silica on the reactivity of activated persulfate for degradation of acid orange 7. *Chemical Engineering Journal* **237**, 487–496.

Liang, C. & Su, H. 2009 Identification of sulfate and hydroxyl radicals in thermally activated persulfate. *Industrial & Engineering Chemistry Research* **48** (11), 5558–5562.

Lin, T., Yu, L., Sun, M., Cheng, G., Lan, B. & Fu, W. 2016 Mesoporous α-MnO 2 microspheres with high specific surface area: Controlled synthesis and catalytic activities. *Chemical Engineering Journal* **286**, 114–121.

Liu, H., Li, G., Qu, J. & Liu, H. 2007 Degradation of azo dye Acid Orange 7 in water by Fe-0/granular activated carbon system in the presence of ultrasound. *Journal of Hazardous Materials* **144** (1–2), 180–186.

Lu, C., Qi, L., Yang, J., Zhang, D., Wu, N. & Ma, J. 2004 Simple template-free solution route for the controlled synthesis of Cu (OH)2 and CuO nanostructures. *Journal of Physical Chemistry B* **108**, 17825–17831.

Masarwa, M., Cohen, H., Meyerstein, D., Hickman, D. L., Bakac, A. & Espenson, J. H. 1988 Reactions of low-valent transition-metal complexes with hydrogen peroxide. Are they Fenton-like or not. 1. The case of Cu/sup +//sub aq/ and Cr/sup 2 +//sub aq/. *Journal of the American Chemistry Society* **110**, 13.

Min, Y., Zhang, K., Chen, Y. & Zhang, Y. 2012 Sonodegradation and photodegradation of methyl orange by InVO4/TiO2 nanojunction composites under ultrasonic and visible light irradiation. *Ultrasonics Sonochemistry* **19** (4), 883–889.

Mondragon, R., Julia, E., Barba, A. & Jarque, J. C. 2012 Characterization of silica-water nanofluids dispersed with an ultrasound probe: a study of their physical properties and stability. *Powder Technology* **224**, 138–146.

Neta, P., Huie, R. E. & Ross, A. B. 1988 Rate constants for reactions of inorganic radicals in aqueous-solution. *Journal of Physical & Chemical Reference Data* **17** (3), 1027–1284.

Nfodzo, P. & Choi, H. 2011 Triclosan decomposition by sulfate radicals: effects of oxidant and metal doses. *Chemical Engineering Journal* **174** (2–3), 629–634.

Oh, S. Y., Kim, H., Park, J., Park, H. & Yoon, C. 2009 Oxidation of polyvinyl alcohol by persulfate activated with heat, Fe^{2+}, and zero-valent iron. *Journal of Hazardous Materials* **168**, 345–351.

Peluffo, M., Pardo, F., Santos, A. & Romero, A. 2016 Use of different kinds of persulfate activation with iron for the remediation of a PAH-contaminated soil. *Science of the Total Environment* **563**, 649–656.

Peng, B., Song, T., Wang, T., Chai, L., Yang, W., Li, X., Li, C. & Wang, H. 2016 Facile synthesis of Fe_3O_4@$Cu(OH)_2$ composites and their arsenic adsorption application. *Chemical Engineering Journal* **299**, 15–22.

Rastogi, A., Ai-Abed, S. R. & Dionysiou, D. D. 2009 Sulfate radical-based ferrous-peroxymonosulfate oxidative system for PCBs degradation in aqueous and sediment systems. *Applied Catalysis B-Environmental* **85** (3–4), 171–179.

Rosenfeldt, E. J. & Linden, K. G. 2004 Degradation of endocrine disrupting chemicals bisphenol A, ethinyl estradiol, and estradiol during UV photolysis and advanced oxidation processes. *Environmental Science & Technology* **38** (20), 5476–5483.

Sharma, V. K. & Millero, F. J. 1988 Oxidation of copper(I) in seawater. *Environmental Science & Technology* **22** (7), 768–771.

Shimizu, N., Ogino, C., Dadjour, M. F. & Murata, T. 2007 Sonocatalytic degradation of methylene blue with TiO_2 pellets in water. *Ultrasonics Sonochemistry* **14** (2), 184–190.

Spanggord, R. J., Yao, D. & Mill, T. 2000 Kinetics of aminodinitrotoluene oxidations with ozone and hydroxyl radical. *Environmental Science & Technology* **34** (3), 450–454.

Suslick, K. S. 1990 Sonochemistry. *Science* **247** (4949), 1439–1445.

Wang, R. 2008 Influence of ultrasound on pitting corrosion and crevice corrosion of SUS304 stainless steel in chloride sodium aqueous solution. *Corrosion Science* **50** (2), 325–328.

Wang, X., Wang, L., Li, J., Qiu, J., Cai, C. & Zhang, H. 2014 Degradation of Acid Orange 7 by persulfate activated with zero valent iron in the presence of ultrasonic irradiation. *Separation and Purification Technology* **122**, 41–46.

Wang, C., Gao, J. & Gu, C. 2017 Rapid destruction of tetrabromobisphenol A by iron(III)-tetraamidomacrocyclic ligand/layered double hydroxide composite/H_2O_2 system. *Environmental Science & Technology* **51** (1), 488–496.

Wang, C., Guo, Z., Hong, R., Gao, J., Guo, Y. & Gu, C. 2018 A novel method for synthesis of polyaniline and its application for catalytic degradation of atrazine in a Fenton-like system. *Chemosphere* **197**, 576–584.

Yan, W., Yan, W., Herzing, A. A., Kiely, C. J. & Zhang, W. 2010 Nanoscale zero-valent iron (nZVI): aspects of the core-shell structure and reactions with inorganic species in water. *Journal of Contaminant Hydrology* **118** (3–4SI), 96–104.

Yuan, R., Yuan, R., Ramjaun, S. N., Wang, Z. & Liu, J. 2011 Effects of chloride ion on degradation of Acid Orange 7 by sulfate radical-based advanced oxidation process: implications for formation of chlorinated aromatic compounds. *Journal of Hazardous Materials* **196**, 173–179.

Yuan, X., Yuan, X., Pham, A. N., Xing, G., Rose, A. L. & Waite, T. D. 2012 Effects of pH, chloride, and bicarbonate on Cu(I) oxidation kinetics at circumneutral pH. *Environmental Science & Technology* **46** (3), 1527–1535.

Zhou, P., Liu, B., Zhang, J., Zhang, Y., Zhang, G., Wei, C., Liang, J., Liu, Y. & Zhang, W. 2016 Radicals induced from peroxomonosulfate by nanoscale zero-valent copper in the acidic solution. *Water Science & Technology* **74**, 1946–1952.

Zou, J., Ma, J., Chen, L., Li, X., Guan, Y., Xie, P. & Pan, C. 2013 Rapid acceleration of ferrous iron/peroxymonosulfate oxidation of organic pollutants by promoting Fe(III)/Fe(II) cycle with hydroxylamine. *Environmental Science & Technology* **47** (20), 11685–11691.

Zou, X., Zou, X., Zhou, T., Mao, J. & Wu, X. 2014 Synergistic degradation of antibiotic sulfadiazine in a heterogeneous ultrasound-enhanced Fe-0/persulfate Fenton-like system. *Chemical Engineering Journal* **257**, 36–44.

First received 15 February 2018; accepted in revised form 6 May 2018. Available online 31 May 2018